Thermochimica Acta 507–508 (2010) 84–90

Contents lists available at ScienceDirect

Thermochimica Acta

journal homepage: www.elsevier.com/locate/tca

Thermogravimetric analysis of selected coal-bearing strata kaolinite

Hongfei Cheng[a,b,c], Qinfu Liu[a], Jing Yang[c], Ray L. Frost[c,*]

[a] School of Geoscience and Surveying Engineering, China University of Mining and Technology, Beijing 100083, China
[b] School of Mining Engineering, Inner Mongolia University of Science and Technology, Baotou 014010, China
[c] School of Physical and Chemical Sciences, Queensland University of Technology, 2 George Street, GPO Box 2434, Brisbane, Queensland 4001, Australia

ARTICLE INFO

Article history:
Received 1 March 2010
Received in revised form 12 April 2010
Accepted 17 May 2010
Available online 24 May 2010

Keywords:
Thermal analysis
Thermogravimetry
Coal-bearing
Kaolinite
Infrared emission spectroscopy

ABSTRACT

Two kinds of coal-bearing kaolinite from China were analysed by X-ray diffraction (XRD), Thermogravimetric analysis–mass spectrometry (TG–MS), infrared emission spectroscopy. Thermal decomposition occurs in a series of steps attributed to (a) desorption of water at 68 °C for Datong coal-bearing strata kaolinite and 56 °C for Xiaoxian with mass losses of 0.36% and 0.51%, (b) decarbonization at 456 °C for Datong coal-bearing strata kaolinite and 431 °C for Xiaoxian kaolinite, (c) dehydroxylation takes place in two steps at 589 and 633 °C for Datong coal-bearing strata kaolinite and at 507 and 579 °C for Xiaoxian kaolinite. This mineral was further characterised by infrared emission spectroscopy (IES). Well-defined hydroxyl stretching bands at around 3695, 3679, 3652 and 3625 cm^{-1} are observed. At 650 °C all intensity in these bands is lost in harmony with the thermal analysis results. Characteristic functional groups from coal are observed at 1918, 1724 and 1459 cm^{-1}. The intensity of these bands decrease by thermal treatment and is lost by 700 °C.

1. Introduction

Kaolinite-rich mineral deposits are very abundant in the Permo-Carboniferous coal-bearing strata of North China and are widely used [1]. It was found that kaolinite usually existed in the upper part of sedimentary cycle, deposited vertically, which was formed in the hydrodynamic environment from strong to weak [2]. Some deposits have high carbon content and form hard minerals. Almost all coal measures of Northern China contain the industrial kaolinite rocks which generally contain a significant amount of organic compounds. The color of coal-bearing kaolinite is rather dark, varying from light gray to gray black to almost completely black [1–3]. In recent years, different researchers have put forward a number of classification programs for the coal-measures kaolinite minerals. The further study of coal-measures kaolinite bearing minerals, based on different factors, such as the material sources, creation environment, late reformation, and industrial value. It is concluded that the sedimentary alteration of volcanic ash may be the main formation mode of kaolinite coal-bearing minerals, but not the only one [3].

The thermal transformation of kaolinite has been investigated by Brown et al. [4,5], He et al. [6] and others [7–12]. The coal-bearing kaolinite rocks are often finely ground and calcined at 950 °C. At this temperature kaolinite is transformed to metakaolinite. It is generally agreed that kaolinite forms metakaolinite by heating in the temperature range 550–950 °C and mullite mainly forms at temperatures above 1150 °C. Mullite is an important constituent in refractories, whitewares and structural clay products when kaolinite is frequently used as the raw material [13]. Therefore, the calcination of coal-bearing kaolinite minerals has been used to prepare mullite.

The calcined kaolin is often used in the rubber and plastic, ceramic raw material, fiberglass, cracking catalysts, cosmetics, medicines and other polymers [14–17]. Properties of calcined kaolin, particularly important for industrial applications, are thermal stability and whiteness [16,18]. Thus, this study of the thermal stability of coal-bearing strata kaolinite rocks is of great important in calcined kaolin industrial applications. The thermal analysis of coal-bearing strata kaolinite also gives new insights not only about improvement of the properties but also serves to protect the environment.

In current study, to the best of the authors' knowledge no thermoanalytical studies of the thermal stability of coal-bearing kaolinite have been undertaken; although differential thermal analysis of some related minerals has been published [19–23]. This paper reports the thermal analysis of two coal-bearing strata kaolinite using XRD, TG-MS and infrared emission spectroscopy.

2. Experimental methods

2.1. Materials

The raw materials used in this work are tonstein, which are kaolinite claystone of volcanic origin found as partings in coal

* Corresponding author. Tel.: +61 7 3138 2407; fax: +61 7 3138 1804.
E-mail address: r.frost@qut.edu.au (R.L. Frost).

0040-6031/$ – see front matter © 2010 Elsevier B.V. All rights reserved.
doi:10.1016/j.tca.2010.05.004

Table 1
Kaolin samples.

Kaolin sample	Location	Content of kaolinite	Particle size	Impurities
Kaolinite (Kd)	Shanxi Datong, China	97%	−45 μm	Quartz
Kaolinite (Kx)	Anhui Xiaoxian, China	93%	−45 μm	Quartz

seams of Permo-Carboniferous strata in Datong (Kd) coal mines from Shanxi province in North China and Permo-Carboniferous strata in Xiaoxian (Kx) from Anhui province in China (Table 1). The beds of Datong coal-bearing kaolinite are about 0.5 m thick and are widespread in the coal-bearing strata of the Datong coalfield. The kaolinite content in the rocks is up to 95% and the quality is very good for industrial use.

2.2. X-ray diffraction

X-ray diffraction patterns were collected using a PANalytical X'Pert PRO X-ray diffractometer (radius: 240.0 mm). Incident X-ray radiation was produced from a line focused PW3373/10 Cu X-ray tube, operating at 40 kV and 40 mA, with Cu Kα radiation of 1.540596 Å. The incident beam passed through a 0.04 rad soller slit, a 1/2° divergence slit, a 15 mm fixed mask, and a 1° fixed antiscatter slit.

2.3. Thermogravimetric analysis and mass spectrometric

Thermogravimetric analysis (TG) of the samples was carried out in a TA® Instruments incorporated high-resolution thermo gravimetric analyser (series Q500) in a flowing nitrogen atmosphere (60 cm^3 min^{-1}). Approximately 50 mg of each sample underwent thermal analysis, with a heating rate of 5 °C/min, with resolution of 6, from 25 to 1000 °C. The TG instrument was coupled to a Balzers (Pfeiffer) mass spectrometer for gas analysis. Only water vapour, carbon dioxide, and oxygen were analysed using mass spectrometry.

2.4. Infrared emission spectroscopy

FTIR emission spectroscopy was carried out on a Nicolet Nexus 870 FTIR spectrometer, which was modified by replacing the IR source with an emission cell. A description of the cell and principles of the emission experiment have been published elsewhere [24–28]. Approximately 0.2 mg of coal-bearing strata kaolinite was spread as a thin layer on a 6 mm diameter platinum surface and held in an inert atmosphere within a nitrogen-purged cell during heating. The infrared emission cell consists of a modified atomic absorption graphite rod furnace, which is driven by a thyristor-controlled AC power supply capable of delivering up to 150 A at 12 V. A platinum disk acts as a hot plate to heat the coal-bearing strata kaolinite sample and is placed on the graphite rod. An insulated 125-μm type R thermocouple was embedded inside the platinum plate in such a way that the thermocouple junction was less than 0.2 mm below the surface of the platinum. Temperature control of ±2 °C at the operating temperature of the sample was achieved by using a Eurotherm Model 808 proportional temperature controller, coupled to the thermocouple.

In the normal course of events, three sets of spectra are obtained over the temperature range selected and at the same temperatures; those of the black body radiation, the platinum plate radiation, and the platinum plate covered with the sample. Normally only one set of black body and platinum radiation is required. The emission spectrum at a particular temperature was calculated by subtraction of the single beam spectrum of the platinum backplate from that of the platinum covered with the sample, and the result ratioed to the single beam spectrum of an approximate black body (graphite). This spectral manipulation is carried out after all the spectral data has been collected.

The emission spectra were collected at intervals of 50 °C over the range 100–1000 °C. The time between scans (while the temperature was raised to the next hold point) was approximately 100 s. It was considered that this was sufficient time for the heating block and the powdered sample to reach temperature equilibrium. The spectra were acquired by co-addition of 128 scans for the whole temperature range, with an approximate scanning time of 1 min, and a nominal resolution of 4 cm^{-1}. Good quality spectra can be obtained providing the sample thickness is not too large. If too large a sample is used then the spectra become difficult to interpret due to the presence of combination and overtone bands. Spectral manipulation such as baseline adjustment, smoothing and normalization was performed using the Spectra calc software package (Galactic Industries Corporation, NH, USA).

3. Results and discussion

3.1. X-ray diffraction (XRD) and chemical composition

The XRD patterns of the two coal-bearing strata kaolinites together with standard XRD pattern are shown in Fig. 1. The XRD patterns of the kaolinites show identical patterns to the standard. The XRD patterns of these two kaolinite minerals show an impurity of quartz. The degree of structural disorder of the coal-bearing strata kaolinite samples can be evaluated on the basis of the XRD background in the range $2\theta = 20–30°$, and the width of the (0 0 2) diffraction peak $d = 0.358$ nm at half the maximum height [29–32]. The intensity of coal-bearing kaolinite in the d (0 2 2), $d(1\bar{3}0)$, $d(\bar{1}31)$, d(0 0 3), $d(1\bar{3}1)$ and $d(\bar{1}13)$ peak suggest that the kaolinite is low defect kaolinite. Structural order in these samples was estimated using the Hinckley index (HI) [30]. The samples from two different area clearly revealed an increase in the ordering in the sense Kx = 1.03 < Kd = 1.35.

The chemical composition of the two coal-bearing strata kaolinite is reported in Table 2. The result shows the two coal-bearing

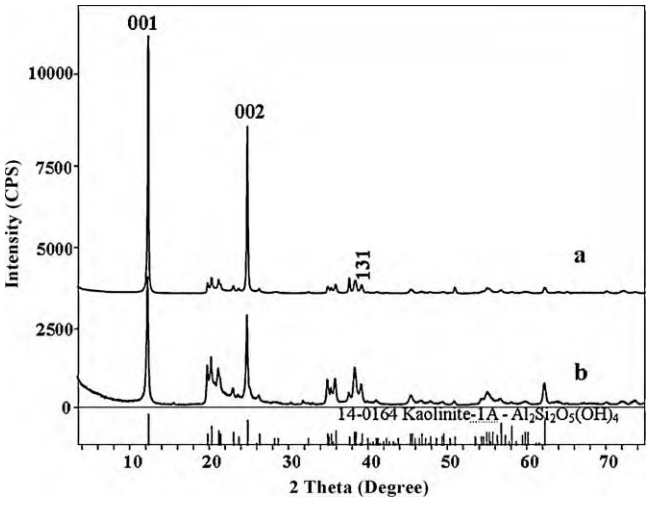

Fig. 1. The XRD patterns of coal-bearing strata kaolinite (a) Kd and (b) Kx.

Table 2
The chemical composition of the coal-bearing kaolinites.

Samples	SiO_2	Al_2O_3	TFe_2O_3	MgO	CaO	Na_2O	K_2O	TiO_2	P_2O_5	MnO	LOT
Taiyuan	53.54	30.13	1.52	1.33	0.39	0.72	0.60	0.12	<0.1	0.065	11.61
Xiaoxian	62.36	27.54	0.88	0.63	0.05	0.11	0.64	0.04	<0.1	0.117	6.91

strata kaolinite including more SiO_2 than general kaolinite about 45%, especially in Xiaoxian kaolinite rock.

3.2. Thermogravimetric analysis and mass spectrometric analysis

Kaolinite is a hydrous layer silicate clay mineral. The structural unit of kaolinite consists of a Si–O tetrahedral sheet and an Al-O(OH) octahedral sheet [33]. Kaolinite is transformed to metakaolinite as the structural water is driven off at temperatures from 550 to 950 °C [1]. It is reported that two main thermal induced processes take place for kaolinite. The whole process can be mostly described by the reaction [13,34–40]:

$$Al_2O_3 \cdot 2SiO_2 \cdot 2H_2O \overset{450-700\ ^\circ C}{\longrightarrow} Al_2O_3 \cdot 2SiO_2 + 2H_2O_{(g)} \quad (1)$$

$$2(Al_2O_3 \cdot 2SiO_2) \overset{925-1050\ ^\circ C}{\longrightarrow} 2Al_2O_3 \cdot 3SiO_2 + SiO_2 \quad (2)$$

The phase transformations are expressed in the form of chemical reactions for the ease of explanation. However, the above equations are unable to describe the coal-bearing strata kaolinite exactly. It is influenced by the degree of disorder of the kaolinite structure, formation environment and the amount and kind of impurities [8,34,41–43].

The thermogravimetric and differential thermogravimetric analysis of coal-bearing strata kaolinite are shown in Fig. 2. The associated mass spectrometric analysis is reported in Fig. 3. The first small mass loss is observed at 68 °C for Kd and 56 °C for Kx and the mass loss is 0.36% and 0.51%. These two mass loss steps are attributed to desorption of adsorbed water.

A second mass loss step is observed at 456 °C for Datong coal-bearing strata kaolinite and 431 °C for Xiaoxian, which was indicated by MS to be the release of CO_2 from coal (Figs. 2 and 3). Yang et al. proposed a set of steps for the dehydration and hydrocarbon of coal and organic from coal-bearing strata kaolinite [44]. These steps correspond to (a) the loss of carbon (b) the loss of organic. Such a scheme is represented by the following chemical equation:

$$C + O_2 \rightarrow CO_2 \quad (3)$$

$$C_mH_n + (2m + \tfrac{1}{2})O_2 \overset{400-500\ ^\circ C}{\longrightarrow} mCO_2 \uparrow + \tfrac{1}{2}nH_2O \uparrow \quad (4)$$

When coal-bearing strata kaolinite lose their so-called "structural water", OH radicals in the structure react together to form water, and the process may be represented by an equation of the

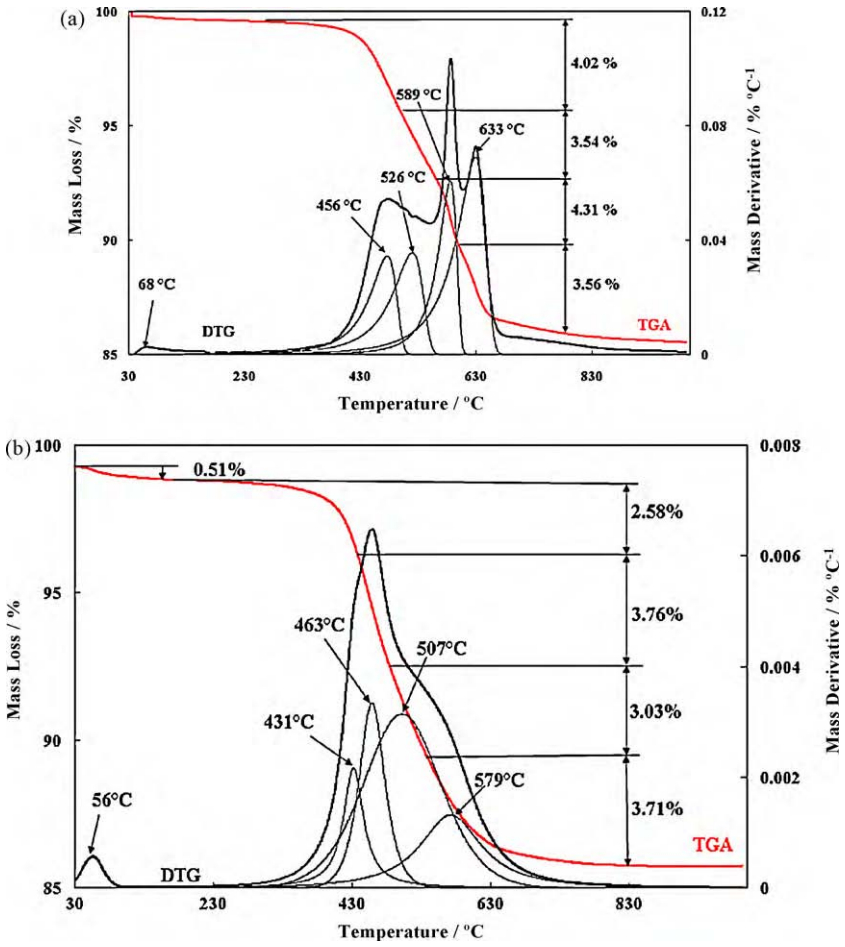

Fig. 2. TGA–DTG curves of coal-bearing kaolinite (a) Kd and (b) Kx.

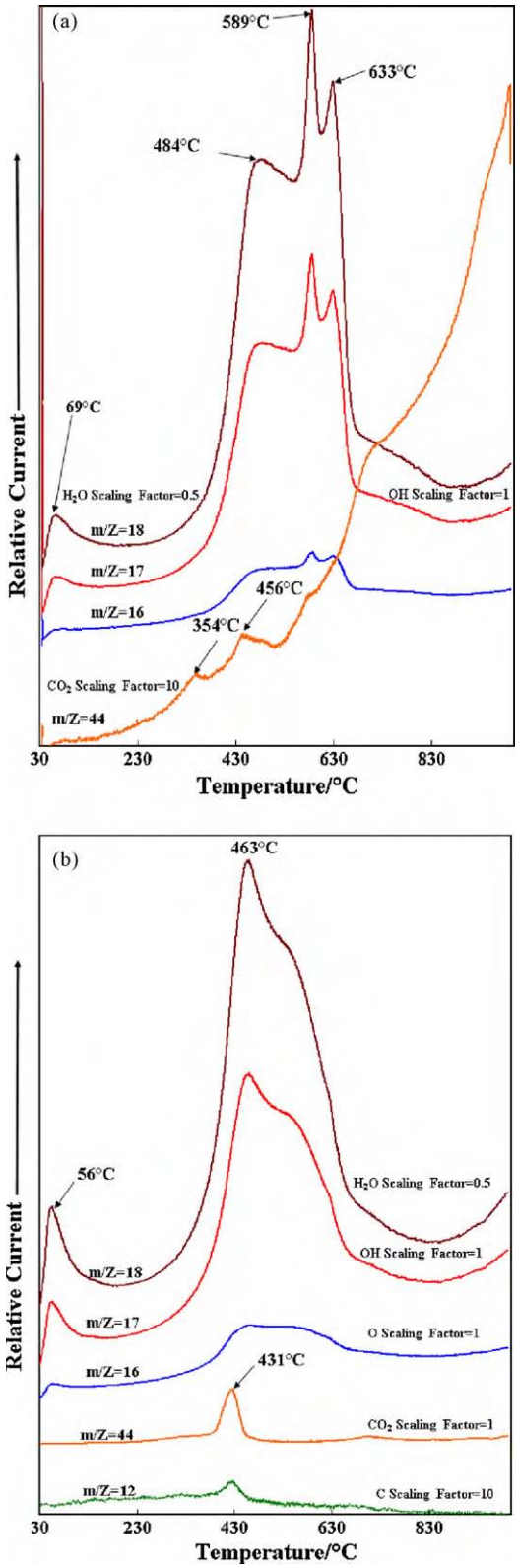

Fig. 3. Evolved gas analysis for coal-bearing kaolinite (a) Kd and (b) Kx.

type [7,38]

$$OH + OH \leftrightarrow H_2O \uparrow + O \quad (5)$$

It is obvious that the mainly dehydration reaction has three stages. The mass loss step is observed at 526 °C for Kd and 463 °C for Kx with mass loss of 3.54 and 3.76%, which is attributed to the decomposition of hydrocarbon from coal. The another mass loss steps occur around 589 °C for Kd and 507 °C for Kx with a mass loss of 4.3% and 3.03%. These mass loss steps are assigned to the dehydroxylation of inner surface OH units. The last mass loss of 3.56% at 633 °C for Kd and 3.71% at 579 °C for Kx are observed, which are attributed to the water release from the octahedral coordinated Al^{3+} ion could generate isolated OH groups or inner hydroxyl units [38,45]. Heating the coal-bearing strata kaolinite results in a loss of hydroxyls. Subsequent exposure to the air results in water being adsorbed and a layer of hydroxyls formed on the surface of metakaolinite [1].

The mass spectrometric gas-release studies can be used to study simultaneously the composition of evolved gases during the thermal treatment [38]. It is well known that the chemical composition of kaolinite is $Al_2Si_2O_5$ $(OH)_4$. In accordance with former findings no distinct stage of dehydration has occurred (at about 450 °C). However, this is unable describe the decomposition of coal-bearing strata kaolinite exactly. Because most of coal-bearing strata kaolinite in China contains a certain amount of organic. In order to clarify the decomposition mechanism of coal-bearing strata kaolinite, the mass loss during each decomposition process should be characterized by the identified evolution components.

The ion current curves for the evolved gases show for $m/z = 18$ and $m/z = 17$ a mass gain at 68 °C for Kd and 56 °C for Kx (Fig. 3a and b). A further mass gain of water vapour occurs at around 589 °C for Kd and 507 °C for Kx. At these two temperatures OH units are lost from the coal-bearing kaolinite structure. Another ion current curves for the evolved gases show for $m/z = 44$ a mass gain at 456 °C for Kd and 431 °C for Kx, which is attributed to the burning of coal present in coal-bearing strata kaolinite. A further mass gain of CO_2 occurs at about 720 °C, which is assigned to decomposition of little amount carbonate impurity. The mass gain in the MS curves corresponds precisely with the mass loss in the TG curves.

3.3. Infrared emission spectroscopy

Typical infrared emission spectra of coal-bearing strata kaolinite of Kd and Kx are show in Fig. 4. The spectra clearly show the temperature at which the OH groups are lost; in the case of Kd the temperature is 700 °C and Kx is 650 °C. The bands of some organic from coal appear to be lost before the temperature at 700 °C for Kd and 600 °C for Kx. In the 500-700 °C temperature for Kd and 400–600 °C for Kx range a broad spectral feature is observed. In order to follow these thermal decomposition three spectra at 300, 500 and 700 °C were selected for further analysis.

The infrared emission spectra of Kd and Kx in the 3550-3750 cm^{-1} region at 300, 500 and 700 °C are shown in Fig. 5a and b, respectively. The higher wavenumber bands at (ν_1)3695 cm^{-1}, (ν_2)3679 cm^{-1}, (ν_3)3652 cm^{-1} and (ν_5)3625 cm^{-1} for Kd and (ν_1)3695 cm^{-1}, (ν_2)3675 cm^{-1}, (ν_3)3654 cm^{-1} and (ν_5)3625 cm^{-1} for Kx are attributed to the hydroxyl stretching of the inner surface hydroxyl, out-of-phase vibration of the inner surface hydroxyls, the second out-of-phase vibration of the inner surface hydroxyls and inner hydroxyls [12,46–48]. In the 300 °C, the spectrum bands ν_1, ν_2, ν_3 and ν_5 are observed. The 500 °C spectrum of Kd shows a small shift in these bands, which are now observed at 3705, 3673, 3652 and 3625 cm^{-1} and the band ν_1 disappeared for Kx. In the 700 °C spectrum, the four bonds all disappeared.

The infrared emission spectra at 300, 500 and 700 °C for Kd and Kx in the 1400–2000 cm^{-1} range are shown in Fig. 6a and b, respectively. The band separation occurs for coal-bearing strata kaolinite in this spectral region. The band at 1456 cm^{-1} in the 300 °C for Kd

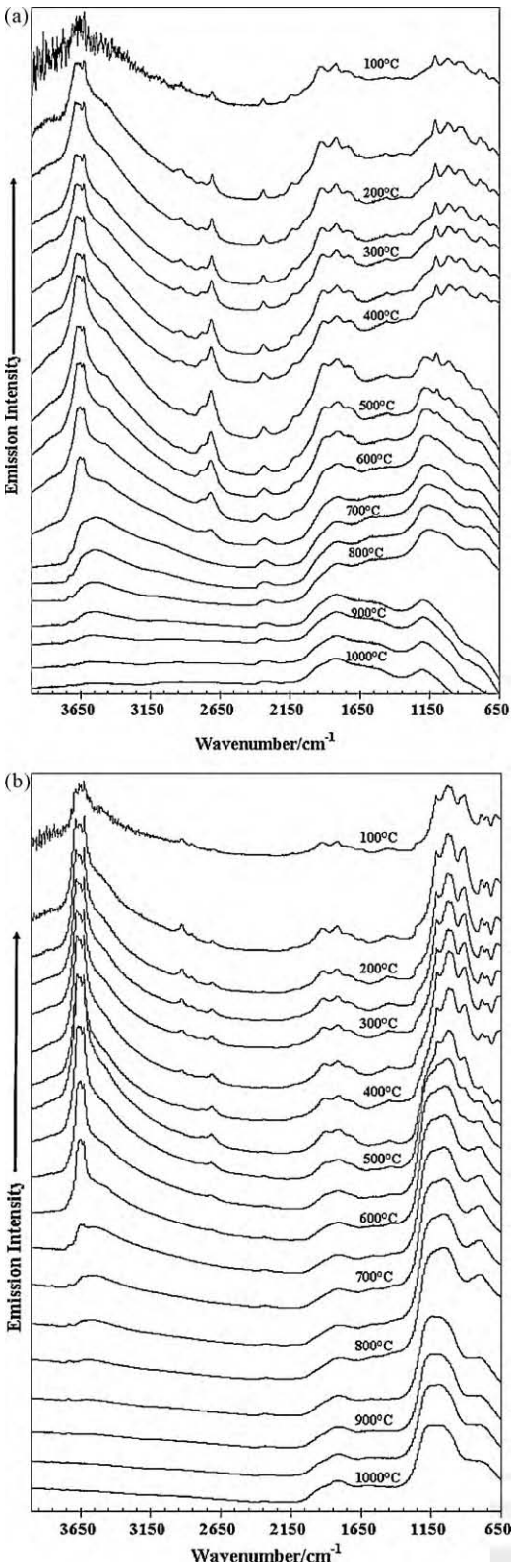

Fig. 4. Infrared emission spectra of coal-bearing kaolinite (a) Kd and (b) Kx over the 100–1000 °C.

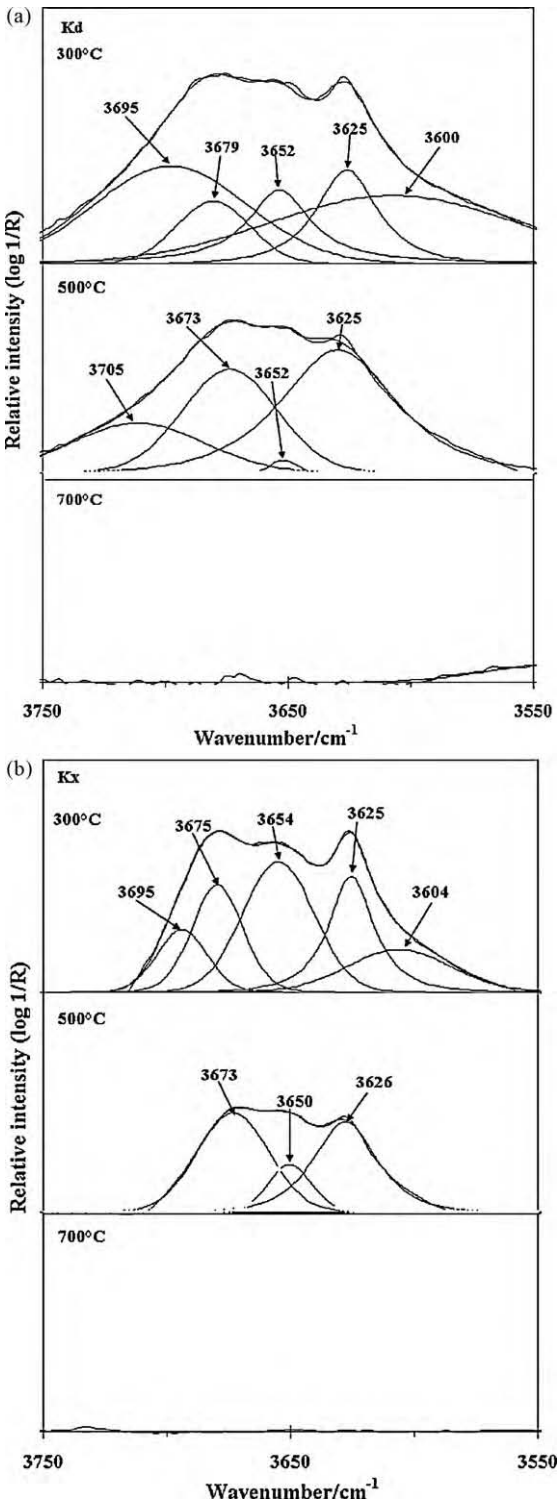

Fig. 5. Infrared spectra of (a) Kd and (b) Kx in the 3550–3750 cm^{-1} region at 300, 500 and 700 °C.

and 1459 cm^{-1} for Kx is attributed to the C=C stretching vibrations, whereas the band at 1710 cm^{-1} for Kd and 1724 cm^{-1} for Kx is assigned to the C=O or COOH stretching vibrations. The band is observed at 1822 cm^{-1} t in the 300 °C for Kd and 1820 cm^{-1} for Kx are attributed to the C–O stretching vibrations. An additional band at 1911 cm^{-1} in the 300 °C for Kd and 1918 cm^{-1} for Kx is observed which is attributed to the C=O vibration [49,50]. These bands are observed for Kd and Kx at 300 °C; at 500 °C the band at 1911, 1710 and 1456 cm^{-1} for Kd and 1915, 1720 cm^{-1} for Kx; and at 700 °C only the band at 1970 cm^{-1}.

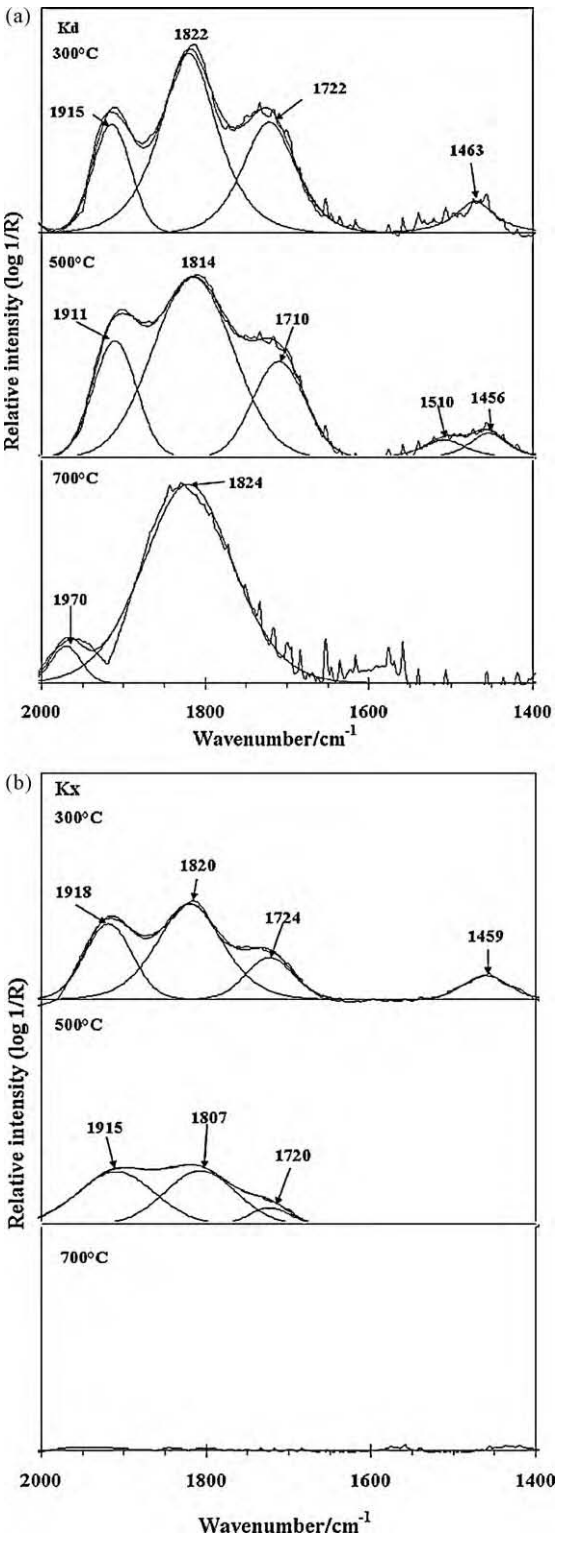

Fig. 6. Infrared spectra of (a) Kd and (b) Kx in the 1400–2000 cm^{-1} region at 300, 500 and 700 °C.

4. Conclusions

The thermal decomposition of two coal-bearing strata kaolinite have been analysed and studied. The temperatures of dehydroxylation and decarbonization found in the coal-bearing kaolinites have been achieved using TG–MS and infrared emission spectroscopy, a very useful technique for determining the thermal decomposition and stability of these minerals. TG–MS and infrared emission spectra show the coal-bearing kaolinite released CO_2 about 450 °C. Thus for protection environment decarbonization before calcination coal-bearing strata kaolinite is necessary.

Acknowledgments

The authors gratefully acknowledge the financial support provided by the National "863" project of China (2008AA06Z109) and infra-structure support of the Queensland University of Technology Inorganic Materials Research Program of the School of Physical and Chemical Science.

References

[1] Q.F. Liu, D.A. Spears, Q.P. Liu, Applied Clay Science 19 (2001) 89–94.
[2] S.L. Ding, Q.F. Liu, Y.Z. Sun, B.H. Xu, World Journal of Engineering 6 (2009) 1–6.
[3] S.L. Ding, Q.F. Liu, M.Z. Wang, Procedia Earth and Planetary Science 1 (2009) 1024–1028.
[4] K.J.D. MacKenzie, I.W.M. Brown, R.H. Meinhold, M.E. Bowden, Journal of the American Ceramic Society 68 (1985) 293–297.
[5] I.W.M. Brown, K.J.D. Mackenzie, M.E. Bowden, R.H. Meinhold, Journal of the American Ceramic Society 68 (1985) 298–301.
[6] H. He, C. Hu, J. Guo, H. Zhang, Chinese Journal of Geochemistry 14 (1995) 78–82.
[7] G.W. Brindley, M. Nakahira, Journal of the American Ceramic Society 40 (1957) 346–350.
[8] J.G. Cabrera, M. Eddleston, Thermochimica Acta 70 (1983) 237–247.
[9] A.D. Gaylord, G.D. Paul, Journal of the American Ceramic Society 57 (1974) 132–135.
[10] J.B. Howard, K. Frank, Journal of the American Ceramic Society 52 (1969) 199–203.
[11] J.S. Killingley, S.J. Day, Fuel 69 (1990) 1145–1149.
[12] R.L. Frost, Clays and Clay Minerals 46 (1998) 280–289.
[13] C.Y. Chen, G.S. Lan, W.H. Tuan, Ceramics International 26 (2000) 715–720.
[14] F. Franco, L.A. Pérez-Maqueda, J.L. Pérez-Rodríguez, Journal of Colloid and Interface Science 274 (2004) 107–117.
[15] X. Zhang, D. Fan, Z. Xu, Journal of Tongji University (Natural Science) 33 (2005) 1646–1650.
[16] F. Franco, J.A. Cecila, L.A. Pérez-Maqueda, J.L. Pérez-Rodríguez, C.S.F. Gomes, Applied Clay Science 35 (2007) 119–127.
[17] E. Mako, J. Kristof, E. Horvath, V. Vagvolgyi, Journal of Colloid and Interface Science 330 (2009) 367–373.
[18] H.H. Murray, I. Wilson, Applied Clay Mineralogy. Occurrences, Processing and Application of Kaolins, Bentonite, Palygorskite-Sepiolite, and Common Clays, 2007.
[19] D. Galusek, Z. Lences, P. Sajgalik, R. Riedel, Journal of Mining and Metallurgy, Section B: Metallurgy 44 (2008) 35–38.
[20] G. Meng, Z. Xu, X. Qi, W. Yang, Z. Xie, Gongye Cuihua 15 (2007) 1–5.
[21] A. Leszczynska, K. Pielichowski, Journal of Thermal Analysis and Calorimetry 93 (2008) 677–687.
[22] A.J. Locke, W.N. Martens, R.L. Frost, Thermochimica Acta 459 (2007) 64–72.
[23] L.K. Joseph, H. Suja, G. Sanjay, S. Sugunan, V.P.N. Nampoori, P. Radhakrishnan, Applied Clay Science 42 (2009) 483–487.
[24] R.L. Frost, S. Bahfenne, J. Graham, Spectrochimica Acta Part A: Molecular and Biomolecular Spectroscopy 71 (2008) 1610–1616.
[25] R.L. Frost, G.A. Cash, J.T. Kloprogge, Vibrational Spectroscopy 16 (1998) 173–184.
[26] R.L. Frost, J.T. Kloprogge, Spectrochimica Acta Part A: Molecular and Biomolecular Spectroscopy 55 (1999) 2195–2205.
[27] R.L. Frost, M.L. Weier, Thermochimica Acta 406 (2003) 221–232.
[28] R. Frost, D. Wain, Journal of Thermal Analysis and Calorimetry 91 (2008) 267–274.
[29] G. Kakali, T. Perraki, S. Tsivilis, E. Badogiannis, Applied Clay Science 20 (2001) 73–80.
[30] D.N. Hinckley, Clays and Clay Minerals 11 (1963) 229–235.
[31] R. Vigil de la Villa, F. Moisés, S.d.R.M. Isabel, V. Iñigo, G. Rosario, Applied Clay Science 36 (2007) 279–286.
[32] C. He, E. Makovicky, B. Osbaeck, Applied Clay Science 9 (1994) 165–187.
[33] R.L. Frost, Clay Minerals 32 (1997) 65–77.
[34] P. Ptacek, D. Kubatova, J. Havlica, J. Brandstetr, F. Soukal, T. Opravil, Thermochimica Acta 501 (2010) 24–29.
[35] O. Castelein, B. Soulestin, J.P. Bonnet, P. Blanchart, Ceramics International 27 (2001) 517–522.
[36] Y.-F. Chen, M.-C. Wang, M.-H. Hon, Journal of the European Ceramic Society 24 (2004) 2389–2397.
[37] R.L. Frost, H. Erzsébet, M. Éva, K. János, R. Ákos, Thermochimica Acta 408 (2003) 103–113.
[38] K. Heide, M. Foldvari, Thermochimica Acta 446 (2006) 106–112.
[39] S.J. Chipera, D.L. Bish, Clays and Clay Minerals 50 (2002) 38–46.
[40] V. Balek, M. Murat, Thermochimica Acta 282–283 (1996) 385–397.

[41] M. Földvári, Journal of Thermal Analysis and Calorimetry 48 (1997) 107–119.
[42] K. Nahdi, P. Llewellyn, F. Rouquerol, R.J.N.K. Ariguib, M.T. Ayedi, Thermochimica Acta 390 (2002) 123–132.
[43] L. Heller-Kallai, Journal of Thermal Analysis and Calorimetry 50 (1997) 145–156.
[44] X. Yang, S. Hu, X. Chen, P. Zhuo, F. Xiang, Journal of China Coal Society 33 (2008) 566–569.
[45] L. Heller-Kallai, I. Miloslavski, A. Grayevsky, American Mineralogist 74 (1989) 818–820.
[46] R.L. Frost, J. Kristof, E. Mako, E. Horvath, Spectrochimica Acta Part A: Molecular and Biomolecular Spectroscopy 59 (2003) 1183–1194.
[47] R.L. Frost, J. Kristof, G.N. Paroz, J.T. Kloprogge, Journal of Colloid and Interface Science 208 (1998) 216–225.
[48] R.L. Frost, S.J. van der Gaast, Clay Minerals 32 (1997) 471–484.
[49] X. Shu, W. Zuna, J. Xu, L. Ge, Journal of Fuel Chemistry and Technology 24 (1996) 426–433.
[50] Z. Zhu, C. Han, C. Zhang, Journal of Fuel Chemistry and Technology 27 (1999) 335–339.